

REDUCIO! Generating 1024×1024 Video within 16 Seconds using Extremely Compressed Motion Latents

Rui Tian¹ Qi Dai^{2*} Jianmin Bao² Kai Qiu² Yifan Yang²
 Chong Luo² Zuxuan Wu^{1*} Yu-Gang Jiang¹
¹Fudan University ²Microsoft Research

Impressionist style, a yellow rubber duck floating on the waves at sunset. *An aerial shot of a lighthouse standing tall on a rocky cliff, its beacon cutting through the early dawn, waves crashing against the rocks below.*



A wizard waves his wand.

Figure 1. Examples of generated high-resolution videos. *Click the top row images to play the video clips. Best viewed with Adobe Reader.*

Abstract

Commercial video generation models have exhibited realistic, high-fidelity results but are still restricted to limited access. One crucial obstacle for large-scale applications is the expensive training and inference cost. In this paper, we argue that videos contain much more redundant information than images, thus can be encoded by very few motion latents based on a content image. Towards this goal, we design an image-conditioned VAE to encode a video to an extremely compressed motion latent space. This magic Reducio charm enables $64\times$ reduction of latents compared to a common

2D VAE, without sacrificing the quality. Training diffusion models on such a compact representation easily allows for generating 1K resolution videos. We then adopt a two-stage video generation paradigm, which performs text-to-image and text-image-to-video sequentially. Extensive experiments show that our Reducio-DiT achieves strong performance in evaluation, though trained with limited GPU resources. More importantly, our method significantly boost the efficiency of video LDMs both in training and inference. We train Reducio-DiT in around 3.2K training hours in total and generate a 16-frame 1024×1024 video clip within 15.5 seconds on a single A100 GPU. Code released at <https://github.com/microsoft/Reducio-VAE>.

*Corresponding authors.

1. Introduction

The straightforward but surprisingly dangerous charm,
Reducio, cause certain things to shrink.

Miranda Goshawk “Harry Potter” [41]

Recent advances in latent diffusion models (LDMs) [40] for video generation have presented inspiring results [1–5, 36, 51, 59, 62], showing great potential in various applications. Commercial models like Sora [31], Runway Gen-3 [42], Movie Gen [35], and Kling [21] can already generate photorealistic and high-resolution video clips. However, training and deploying such models are computationally demanding—thousands of GPUs and millions of GPU hours are required for training, and the inference for a one-second clip costs several minutes. Such a high cost is becoming a significant obstacle for research and large-scale real-world applications.

Extensive effort has been made to relieve the computational burden by means of efficient computation modules in the backbone [48, 58], optimizing diffusion training strategies [11, 55], and adopting few-step sampling methods [45, 61]. However, in this paper, we argue that the very nature of the problem is long neglected. Concretely, most video LDMs stick to the paradigm of text-to-image diffusion, *e.g.*, Stable Diffusion (SD) [40], and inherently employ the latent space of its pre-trained 2D variational autoencoder (VAE) [20, 38]. This scheme compresses the input videos by $8\times$ in each spatial dimension, which is suitable for images while being much surplus for video.

As videos naturally carry much more redundancy than images, we believe they can be projected into a much more compressed latent space with a VAE based on 3D convolutions. Surprisingly, for videos, a $16\times$ spatial down-sampling factor does not sacrifice much of the reconstruction performance. While the resulting distribution of latent space shifts from those of the pre-trained image LDMs, we can still wield their well-learned spatial prior by factorizing text-to-video generation with a condition frame [10, 52, 57, 65]. In particular, we can obtain a content frame with off-the-shelf text-to-image LDMs and then generate samples with text and image as joint priors into video LDMs.

More importantly, as the image prior delivers enriched spatial information of video contents, factorized video generation offers the potential for further compression. We argue that video can be encoded into very few latents representing motion variables, *i.e.*, motion latents, plus a content image. Hereby, we introduce the magical *Reducio* charm by building a VAE comprised of a 3D encoder that aggressively compresses input videos into a $4096\times$ down-sampled compact space, and a 3D decoder fused with feature pyramids of the middle frame as the content condition. Notably, the resulting *Reducio*-VAE surpasses the common 2D VAE

by 5db in PSNR while using a $64\times$ smaller latent space.

Subsequently, we establish the LDM with a diffusion transformer (DiT) [6, 32]. Besides using T5 features [37] as the text condition, we employ an image semantic encoder as well as a context encoder to provide additional image conditions, which inform the model of the spatial content. Thanks to the extremely compressed video latent, our diffusion model, namely *Reducio*-DiT, thus enjoys both the fast training (inference) speed and high generation quality. Specifically, *Reducio*-DiT achieves 318.5 FVD score on UCF-101, surpassing a bunch of previous work [1, 4, 52, 53, 66] while being much faster. It can also be easily upscaled to a larger resolution, *e.g.* 1024^2 , with affordable cost. Our experiments show that *Reducio*-DiT can generate a 16-frame video clip of 1024^2 resolution within 15.5 seconds on a single A100 GPU, and hence achieves a $16.6\times$ speedup over Lavie [53].

In summary, our contributions are as follows: (1) We encode video into very few motion latents plus a content image, where the designed *Reducio*-VAE can compress video into a $64\times$ smaller latent space compared to common 2D VAE. (2) Based on *Reducio*-VAE, a diffusion model called *Reducio*-DiT is devised by incorporating additional image conditions. (3) Experiments show that our *Reducio*-DiT can significantly speed up the generation process while producing high-quality videos.

2. Related Work

Video diffusion models have become the latest craze in the field of text-to-video generation. Due to the huge success of text-to-image LDMs [14, 27, 28, 40, 44], attempts [3, 4, 51] have been made to leverage the powerful UNet-based stable diffusion models pre-trained in 2D space by inserting temporal convolution and attention layers. Recently, the strong performance of transformers has continued in image generation domain [6, 8, 22] by diffusion transformers (DiT) [32]. Consequently, recent works have focused on extending DiT-based diffusion models from 2D spatial attention to spatiotemporal attention.

While the mainstream exploration [35] follows the paradigm of image diffusion models by using text as the only condition, an emerging stream of works [10, 52, 65] decompose text-to-video diffusion into two steps, *i.e.*, text-to-image and text-image-to-video generation. This factorizing encourages models to concentrate on motion modeling instead of challenging spatiotemporal joint modeling. In this work, we take advantage of factorized text-to-video generation and build our framework upon DiT. Thanks to the delicate structure of *Reducio*-VAE, our model manages to preserve the fine details of image priors in generated videos, and hence can be used for more high-demanding real-world applications, *e.g.*, advertisement generation.

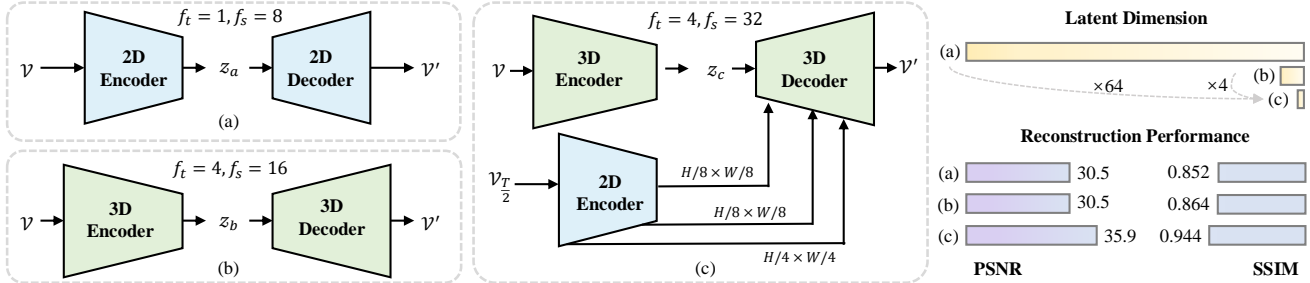


Figure 2. Architecture and performance comparisons between vanilla 2D VAE in (a) SDXL, (b) 3D VAE and (c) the proposed *Reducio*-VAE. *Reducio*-VAE enables 64× reduction of latent size while achieving much higher reconstruction performance.

Efficient diffusion models have gained increasing attention due to the tremendous computational resources and time required for training and inferring samples, especially for high-resolution images and videos. On one hand, researchers have made attempts to build LDMs with more efficient architectures [9, 48, 56, 69]. For example, DIM [48] uses Mamba as its backbone to ease the computational burden compared to vanilla transformers. Another line of work leverages efficient diffusion techniques to perform fewer sampling steps during inference [25, 45, 61] or to accelerate convergence during training [11, 55]. For instance, Stable Diffusion 3 [8] and Flux [22] employ rectified flow [23] for improved training and inference efficiency.

Our work focuses on designing a more compact latent space [33], which straightforwardly and effectively reduces the overall training and inference costs of LDM. PVDM [63] and CMD [64] propose projecting 3D video samples into three separate yet compact 2D latent spaces. However, this approach requires training separate diffusion models for each space, which inevitably leads to discrepancies during inference. Our *Reducio*-VAE takes after LaMD [16] to adopt a factorized, compact motion latent space with the help of a content frame for reconstruction. In contrast, we emphasize aggressive compression of the spatial dimension and suggest that a moderate temporal down-sampling factor provides the best trade-off between performance and efficiency. Concurrent research in the image domain also indicates that using a high spatial down-sampling factor on redundant visual content [47, 56], such as high-resolution images, significantly improves efficiency. We propose that it is crucial to recognize the importance of spatial redundancy in the video latent space.

3. Reducio

3.1. Reducio Video Autoencoder

Variational autoencoder (VAE) [20] projects input images or videos into a compressed latent space obeying a certain distribution and maps the latent sampled from the obtained distribution into RGB space with a decoder. Latent diffusion models [40] take advantage of the down-sampled la-

tent space of VAE to support generation with improved efficiency. In this paper, we follow the common practice and build our video autoencoder upon VAE.

We denote the temporal down-sampling factor of a VAE as f_t and the spatial one as f_s . Given an input video \mathcal{V} with the shape of $3 \times T \times H \times W$, the compressed latent $z_{\mathcal{V}}$ as the input into diffusion models fall into the space of $|z| \times T/f_t \times H/f_s \times W/f_s$, where z denotes the latent channel. Thanks to the superior performance of open-source Stable Diffusion (SD) [40] models, it has been a common practice to leverage SD-VAE to process images and videos into compressed latent. Typically, as shown in (a) of Fig. 2, SD-VAE is built upon 2D convolution with $f_s = 8$ and $f_t = 1$.

Reducio charm on videos. As adjacent video frames share large similarities in pixel space, video signals are inherently more redundant than images. Based on this idea, we adopt a more aggressive down-sampling factor for video autoencoder. Specifically, we inflate the 2D convolutions into 3D convolutions and increase the number of autoencoder blocks, increasing f_t and f_s to 4 and 16, as illustrated in (b) of Fig. 2. While the overall down-sampling factor increases by 16×, the compressed latent space suffices to achieve comparable pixel-space reconstruction performance, making a strong case for the potential of extremely shrinking video latent dimension.

As for image-to-video generation, we argue that video latent can be further compressed as the content image contains rich visual details and substantial overlapping information. In such a scenario, video latents can be further simplified to represent the motion information. We can find similar spirits in video codec [39], where carefully designed modules use reference frames as inputs to perform high-fidelity reconstruction of a given compressed code. Specifically, we propose to cast the *Reducio* charm on video latent space, as shown in (c) of Fig. 2. Generally, we choose the middle frame $V_{T/2}$ as the content guidance, compress input videos by an extreme down-sampling factor with a 3D encoder, and reconstruct from the latent space with the aid of content frame features pyramids. Specifically, we infuse content features of sizes varying in $H/8 \times W/8$ and $H/4 \times W/4$ via cross-attention within the decoder, adopt an

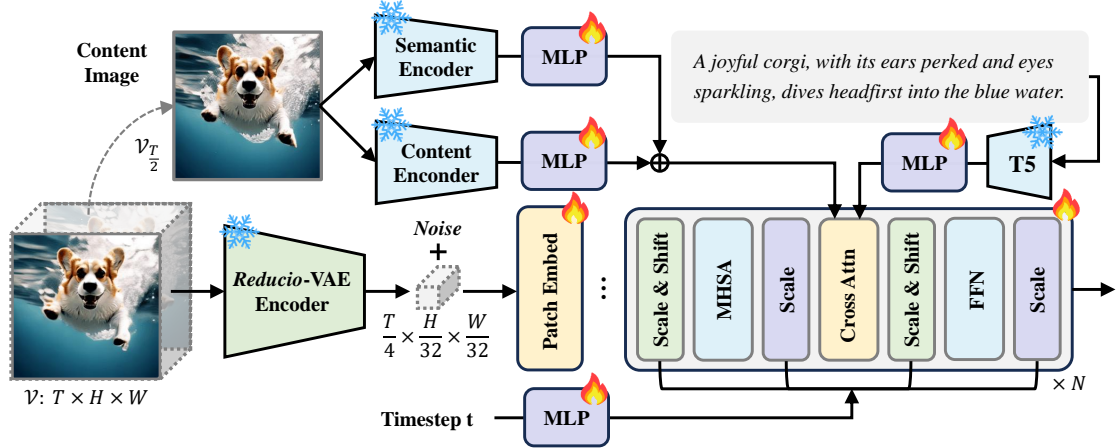


Figure 3. The overview of *Reducio*-DiT training framework. Compared to DiT, *Reducio*-DiT requires an additional image-condition module to inject the semantics and content of the keyframe via cross-attention.

extreme compression ratio, *i.e.*, $f_s = 32$ and $f_t = 4$. While *Reducio*-VAE projects videos into $64\times$ more compressed latent space than one of SDXL-VAE [34], it significantly outperforms the latter in reconstruction performance.

3.2. Reducio Diffusion Transformer

Thanks to the magical compression capability of *Reducio*-VAE, we project input videos into compressed latent space with a down-sampling factor of 4096, and hence significantly speed up the training and inference of diffusion models. In specific, we adopt the DiT-XL [32] model and follow most of the design choices adopted by PixArt- α [6], *i.e.*, AdaLN-single modules, cross attention layers with Flan-T5-XXL [37] text conditions. The training target follows the reverse diffusion process [14], which can be depicted as

$$p_\theta(z_{t-1}|z_t) = \mathcal{N}(z_{t-1}; \mu_\theta(z_t, t), \sigma_t^2 \mathbf{I}), \quad (1)$$

where z is latent, t is time step, $\mu_\theta(z_t, t)$ and σ_t^2 indicate the mean and variance of the sample at the current time step. By re-parameterizing μ_θ as a noise prediction network ε_θ , the model can be trained using simple mean-squared error between the predicted noise $\varepsilon_\theta(z_t, t)$ and the ground truth sampled Gaussian noise ε formulated as

$$\mathcal{L}_{simple} = \mathbb{E}_{z_0, \varepsilon, t} (\|\varepsilon - \varepsilon_\theta(z_t, t)\|^2). \quad (2)$$

To adapt the image diffusion model to video, we consider two options: (1) Directly transforming the 2D attention to full 3D attention, without adding additional parameters. (2) Adding temporal layers and transforming the model to perform 2D spatial attention plus 1D temporal attention. We adopt option (1) by default. Studies on the evaluation of these two options are shown in Sec. 4.3.2.

In addition, to tailor for image-conditioned video generation, we introduce *Reducio*-DiT (illustrated in Fig. 3) with additional image-condition modules, as described below.

Content frame modules consist of a semantic encoder built upon pretrained OpenCLIP ViT-H [7] and a content encoder initialized with the SD2.1-VAE [40]. The former encoder projects content frames into a high-level semantic space while the latter one mainly focuses on extracting the spatial information. We concatenate the obtained features with text tokens output by T5 to form the image-text-joint condition, and then cross-attend them with the noisy video latent. Concretely, the detailed operations can be described as:

$$\begin{aligned} e_s &= \text{OpenCLIP}(V_{T/2}), \\ e_c &= \text{SD-VAE}(V_{T/2}), \\ e_{img} &= \text{MLP}(e_s) \oplus \text{MLP}(e_c), \\ e_p &= \text{MLP}(\text{T5}(\text{prompt})), \\ e &= [e_{img}, e_p], \\ z_i &= \text{CAtn}(z_i, e), \end{aligned} \quad (3)$$

where $V_{T/2}$ is the condition image, \oplus refers to element-wise addition, $[\cdot]$ refers to concatenation, and $\text{CAtn}(\cdot)$ refers to cross-attention.

Scaling up to high-resolution videos consumes tremendous computational resources for vanilla video diffusion models. Nevertheless, *Reducio*-DiT relieves this limit to a great extent. To support high-resolution (*e.g.*, 1024^2) video generation, we employ a progressive training strategy: 1) in the first stage of training, the model learns to align the video latent space with text-image prior by taking in a vast number of 256^2 videos as input; 2) in the second stage, we fine-tune the model on videos with higher resolution, *i.e.*, 512×512 . In consequence, the content encoder augments $4\times$ more tokens with the noisy latent; 3) in the third stage, we conduct further fine-tuning on videos with spatial resolution around 1024 with multi-aspect augmentation.

To better accommodate the model to videos with varying aspect ratios, we inject the aspect ratio and size of input videos as embeddings into the DiT model. Then we add

Table 1. Quantitative comparison with open-source state-of-the-art VAE for generation.

Model	Downsample Factor	$ z $	Pexels				UCF-101	
			PSNR \uparrow	SSIM \uparrow	LPIPS \downarrow	rFVD \downarrow	rFVD \downarrow	
SD2.1-VAE [40]	$1 \times 8 \times 8$	4	29.23	0.82	0.09	25.96	21.00	
SDXL-VAE [34]	$1 \times 8 \times 8$	16	30.54	0.85	0.08	19.87	23.68	
OmniTokenizer [50]	$4 \times 8 \times 8$	8	27.11	0.89	0.07	23.88	30.52	
OpenSora-1.2 [30]	$4 \times 8 \times 8$	16	30.72	0.85	0.11	60.88	67.52	
Cosmos-VAE [29]	$8 \times 8 \times 8$	16	30.84	0.74	0.12	29.44	22.06	
	$8 \times 16 \times 16$	16	28.14	0.65	0.18	77.87	119.37	
Reducio-VAE	$4 \times 32 \times 32$	16	35.88	0.94	0.05	17.88	65.17	

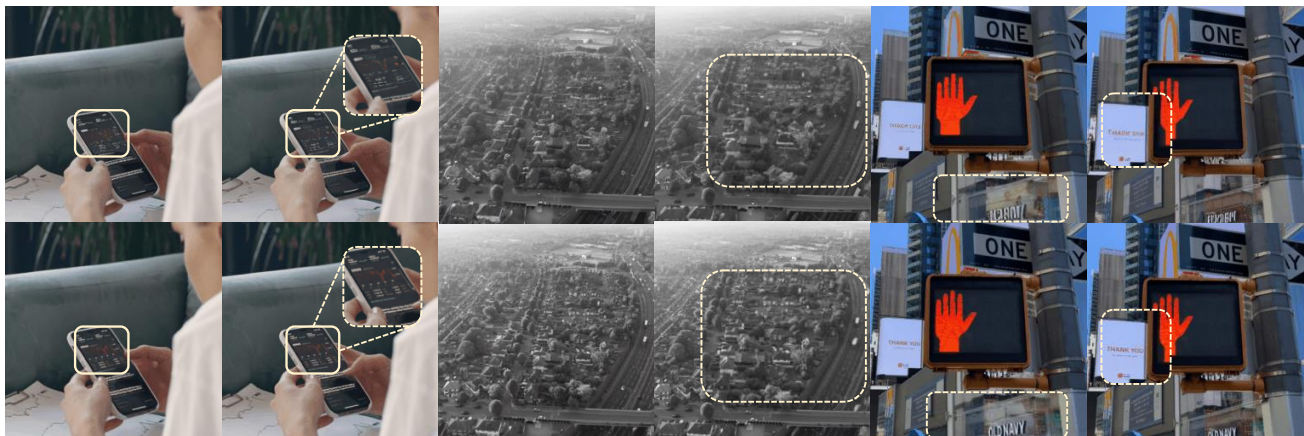


Figure 4. Comparison between the 1st and 16th frames of videos reconstructed by SDXL-VAE (top) and *Reducio*-VAE (bottom).

the dynamic size embedding with timestep embedding before being fed into the MLP. More importantly, for models in the first and the second stages, the content encoder cross-attends $H/16 \times W/16$ tokens with the noisy latent. As computational costs grow rapidly when resolution increases, we introduce a strategy to ensure the efficiency of *Reducio*-DiT on high-resolution videos. Specifically, we aim to shrink the content embedding by $2 \times$ in the spatial dimension in each cross-attention layer. Inspired by Deepstack [26], we divide input tokens into 4 groups of grids and iteratively concatenate each group of $H/32 \times W/32$ tokens with the other condition tokens.

4. Experiments

4.1. Training and Evaluation Details

Our *Reducio*-VAE is trained on a 400K video dataset collected from Pexels*. Pexels contains a large number of free and high-quality stock videos, where each video is accompanied by a short text description. We train *Reducio*-VAE from scratch on 256×256 videos with 16 FPS. Note that we split videos with higher resolutions into tiles in the spatial dimension. To perform the VAE comparison,

*<https://www.pexels.com/>

PSNR, SSIM [54], LPIPS [67] and reconstruction FVD (rFVD) [49] are employed as the evaluation metrics.

Reducio-DiT is trained on the above Pexels dataset and an internal dataset with 5M videos containing high-resolution text-video pairs. As described in Sec. 3.2, we adopt a multi-stage training strategy to train the model from low resolution to high resolution. We first train *Reducio*-DiT-256 using a batch size of 512 on 4 Nvidia A100 80G GPUs for around 900 A100 hours and initialize model weights with PixArt- α -256 [6]. Then we fine-tune on 512^2 videos shortly for 300 A100 hours to obtain *Reducio*-DiT-512. In the third stage, we randomly sample video batches from 40 aspect ratio buckets, which is the same as the setting in PixArt- α . We leverage 8 AMD MI300 GPUs to support a training batch size of 768 and fine-tune *Reducio*-DiT-1024 for 1000 GPU hours.

We adopt DPM-Solver++ [24] as the sampling algorithm for efficient inference and set the sampling step to 20. For evaluation in Tab. 2, we calculate the speed of generating 16-frame video clips on a single A100 80G GPU and denote out-of-memory as OOM. For *Reducio*-DiT, we use PixArt- α -256 and PixArt- α -1024 to generate the content frame for 256^2 and 1024^2 videos, respectively. We report the FVD and IS scores of *Reducio*-DiT-512 under the zero-

Table 2. Quantitative comparison with state-of-the-art video LDMs.

Model	Params	VBench	FVD↓		Throughput (#videos/sec)		GPU Hours A100 Training
			UCF-101	MSR-VTT	256 × 256	1024 × 1024	
Make-A-Video [43]	-	-	367.23	-	-	-	-
CogVideo [15]	7.8B	67.01	701.59	1294	0.0023	OOM	>368K
Show-1 [66]	1.7B	78.93	394.46	538.0	0.0016	OOM	>56K
Lavie [53]	1B	77.08	526.30	-	0.1838	0.0039	-
MicroCinema [52]	2B	-	342.86	377.4	0.0234	OOM	>25K
Lumiere [2]	>2B	-	332.49	-	-	-	-
<i>Reducio</i> -DiT	1.2B	81.39	318.50	291.9	0.9824	0.0650	3.2K



A child excitedly swings on a rusty swing set, laughter filling the air.

Figure 5. Comparison between frames generated given an identical frame and prompt, by (a) DynamicCrafter [57], (b) SVD-XT [3] and (c) *Reducio*-DiT, respectively. We resize the output frames from 1344 × 768 to 1024 × 576 to match with the former two baselines.

shot setting on UCF-101 [46] and MSR-VTT [60]. Since our method is a two-stage video generation approach, which requires a condition image prior, we follow MicroCinema [52] to use SDXL [34] to generate the condition image for all the evaluations, including the FVD on UCF-101 and MSR-VTT. Additionally, we evaluate *Reducio*-DiT-512 on the recent video generation benchmark VBench [17].

4.2. Main Results

***Reducio*-VAE preserves fine details** of video inputs. Fig. 4 displays the first and the last frame of 256² videos reconstructed by SDXL-VAE and *Reducio*-VAE, with the yellow bounding box highlighting the region with obvious differences in details. While SDXL-VAE causes corruptions and blurs, *Reducio*-VAE generally maintains the subtle texture within the middle frame. Tab. 1 also reflects the advantage of *Reducio*-VAE in quantitative reconstruction metrics, e.g., PSNR, SSIM, and LPIPS on a randomly sampled validation subset of 1K videos with the duration of 1s on Pexels, and test on both UCF-101 and Pexels for FVD.

As shown in the table, *Reducio*-VAE strikes obvious ad-

vantages on overall reconstruction performance. Specifically, our model significantly outperforms state-of-the-art 2D VAE, e.g., SD2.1-VAE and SDXL-VAE, by more than 5 db in PSNR. Moreover, *Reducio*-VAE also performs better than VAEs designed for video in recent literature, e.g., OmniTokenizer and OpenSora-1.2. Our VAE also outperforms the concurrent work, Cosmos-VAE, which also adopts a further compressed video latent space, by 0.2 in SSIM and 5 db in PSNR with an 8× higher down-sampling factor.

We observe *Reducio*-VAE has worse rFVD than others on UCF-101. By careful inspection, we find the selected prior content image is blurring in many cases due to the low visual quality of UCF-101 and hence result in a lower reconstruction quality. In contrast, *Reducio*-VAE places first on rFVD on pexels, which consists of videos with much improved visual quality and much higher resolution.

***Reducio*-DiT achieves a promising balance between efficiency and performance.**

As we harness an extremely compressed latent space, the training cost of our diffusion models is similar to the one of the text-to-image diffusion model. With a training cost of merely 3.2K A100 hours,

our model achieves FVD scores of 318.50 on UCF-101 and 291.0 on MSR-VTT and the VBench score of 81.39, beating a range of previous stat-of-the-art video LDMs, as recorded in Tab. 2. Fig. 5 displays the comparison between *Reducio*-DiT and the other two stat-of-the-art image-to-video models. While DynamicCrafter and SVD-XT both fail to generate stable frames consistent with the given content frame, *Reducio*-DiT yields high visual quality with facial details in the content frame uncorrupted.

Moreover, *Reducio*-DiT significantly boosts the throughput of video LDMs. The compressed latent space facilitates *Reducio*-DiT to output 256^2 videos of 16 frames in almost 1 second, which realize a $5.3\times$ speed up compared with Lavie. Moreover, 16-frame 1024^2 video generation costs *Reducio*-DiT only for 15.4 seconds on average, leading to a striking speedup of $16.6\times$ over Lavie. We argue the core philosophy of *Reducio* lies in the extremely compressed latent space, which acts as the key role in accelerating both the training and inference speed of video LDMs.

4.3. Ablation Studies

4.3.1. Design of *Reducio*-VAE

Spatial redundancy is the key for compression. As Tab. 3 displays, when adopting an identical overall down-sampling factor $\mathcal{F} = f_t \cdot f_s^2$, *Reducio*-VAE achieves worse performance with larger compression factor in the temporal dimension. The result suggests that when a reference frame is provided, videos contain heavier redundancy in the spatial dimension than in the temporal dimension. Similarly, when $f_s = 32$ is kept unchanged, increasing f_t from 2 to 4 leads to a drop in PSNR by 0.91 db. To balance the trade-off between more compact latent space and better reconstruction performance, we set $f_t = 4$ and $f_s = 32$ in default.

Table 3. Ablation on the down-sampling factor of *Reducio*-VAE.

f_t	f_s	PSNR \uparrow	SSIM \uparrow
16	16	34.14	0.93
2	32	36.79	0.96
4	32	35.88	0.94
1	64	35.51	0.93

Scaling up latent channel is helpful for improving the reconstruction performance, as results shown in Tab. 4. When z grows from 4 to 16, the PSNR of reconstructed videos increases by 2.71 db. However, increasing the latent channel has a ceiling effect, as setting z to 32 hardly achieves further gains in both PSNR and SSIM. Therefore, we opt to use latent space with $|z| = 16$ for *Reducio* as the default setting. A visual qualitative comparison is presented in Fig. 6, where we compare the results when $|z| = 16, 8,$ and 4.

Fusion with cross-attention achieves the most competitive performance in Tab. 5. As for add-based fusion, we feed the

Table 4. Ablation on latent channel dimensions of *Reducio*-VAE.

$ z $	PSNR \uparrow	SSIM \uparrow
4	33.17	0.91
8	34.15	0.93
16	35.88	0.94
32	35.24	0.94



Figure 6. Comparison between the 8th to 11th frames of videos reconstructed by *Reducio*-VAE with different latent space channel dimensions, i.e., (a) $|z| = 16$, (b) $|z| = 8$, (c) $|z| = 4$.

content frame features into a convolution and replicate the output on the temporal dimension. Then we add video features with the content feature, together with a temporal embedding. Concerning linear-based fusion, we view the content condition as a single-frame video feature and concatenate it with the video feature by the temporal dimension. A 3D convolution layer then refines the concatenated features. As observed in Tab. 5, the attention-based *Reducio*-VAE outperforms other baselines by 1.71 in PSNR and 0.01 in SSIM, while demanding higher computational costs. By default, we display results using the attention-based fusion. Note that all *Reducio*-VAE displayed in Tab. 5 share the same 3D encoder and hence an identical latent space, where users are free to choose any of the decoders with different resource constraints.

Table 5. Ablation on the fusion type in *Reducio*-VAE when infusing the content image.

Fusion	PSNR \uparrow	SSIM \uparrow	Params
w/o.	27.91	0.80	435M
linear	30.86	0.87	439M
add	34.17	0.93	450M
attention	35.88	0.94	437M

4.3.2. Design of *Reducio*-DiT

For ablation studies on DiT, we conduct training for 300 A100 hours for each experiment on Pexels and report FVD and IS scores on UCF-101.

Using patch size of one yields the best performance. As shown in Tab. 6, keeping a fixed spatial down-sampling factor of 32, we compare the performance of using a $2\times$ higher temporal down-sampling factor in latent space and a temporal patch size of 1 ($f_t = 4, p_t = 1$), with temporal patch size of 2 when patchify the input latents for obtaining patch embedding ($f_t = 2, p_t = 2$). We observe that compressing the temporal dimension with VAE outperforms. Similarly, we ablate using VAE with $2\times$ lower spatial down-sampling factor yet setting the patch size of spatial dimension to 2 ($f_s = 16, p_s = 2$). The experimental results identify that compressing the video with *Reducio*-VAE to an extreme extent and using a small patch size, *i.e.*, 1, in both the temporal and spatial dimensions achieves better performance.

Table 6. Ablation on the temporal patch size p_t and the spatial patch size p_s in *Reducio*-DiT.

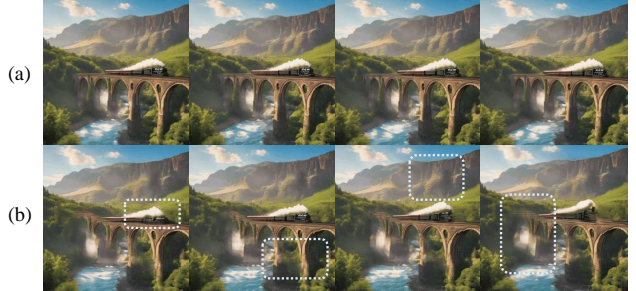
f_t	f_s	p_t	p_s	FVD↓	IS↑
2	32	2	1	351.0	32.7
4	16	1	2	534.1	30.4
4	32	1	1	337.6	34.1

Using joint spatiotemporal attention (3D attention) outweighs using factorized spatial and temporal attention (*i.e.*, 2D + 1D attention) in generation quality. Interestingly, we observe that factorized attention leads to a faster convergence of training loss. However, with the same training step, as shown in Tab. 7, factorized attention lags behind its counterpart with joint 3D attention for 45 in FVD. We suppose the possible reason is that 2D + 1D scheme demands adding additional temporal layers and performs factorized self-attention on a small set of tokens each, making it hard to model smooth open-set motion with the light computation. In contrast, 3D attention directly exploits the original parameters and collaborates all spatiotemporal tokens.

Table 7. Ablation on the attention type in *Reducio*-DiT.

Attn	FVD↓	IS↑
2d + 1d	382.2	32.4
3d	337.6	34.1

Fusion with both semantic and content information contributes to the best quality. As shown in Tab. 8, using semantic features, *i.e.*, OpenClip-based features alone may contribute to distorted visual detail, leading to a lower FVD. on the other hand, using content-based features helps to



A stunning sight as a steam train leaves the bridge, traveling over the arch-covered viaduct. The landscape is dotted with lush greenery and rocky mountains.

Figure 7. Comparison on conditioning type in *Reducio*-DiT. (a) using semant.+content features. (b) using semantic features only.

make video smooth and stable, achieving a higher FVD yet less versatile motion. A comparison example is illustrated in Fig. 7. The collaboration of content and semantic features helps *Reducio* strike the best balance between content consistency and motion richness.

Table 8. Ablation on the conditioning type in *Reducio*-DiT.

Condition	FVD↓	IS↑
semantic	472.1	34.5
content	363.7	31.1
semantic + content	337.6	34.1

5. Conclusion

Video generation has shown promising results with many potential applications, but is still trapped by the unaffordable computation cost. In this paper, we explored how to effectively cut the overhead by reducing the latent size. Particularly, we found the video can be encoded into extremely compressed latents with the help of a content image prior, where the latent codes only need to represent the motion variables. With this observation, we designed the *Reducio*-VAE to compress videos to $4096\times$ smaller latents. Using this powerful *Reducio*-VAE, we trained the *Reducio*-DiT that enables fast high-resolution video generation. Our method is also compatible with other accelerating techniques, *e.g.* rectified flow, allowing for further speedup, where we leave it for future exploration.

Limitations and future work. While *Reducio*-DiT shows a strong capacity of being consistent with the center frame, the generated videos are still relatively short (16 frames of 16 fps, *i.e.*, 1 second) for real-world applications. Given the length of the video, the magnitude of the motion is also somehow limited in generated videos. We believe in the potential of adapting our works for longer video generation and will explore it as the future work.

Reducio is purely a research project. Currently, we have no plans to incorporate *Reducio* into a product or expand ac-

cess to the public. We will also put Microsoft AI principles into practice when further developing the models. In our research paper, we account for the ethical concerns associated with text-image-to-video research. To mitigate issues associated with training data, we have implemented a rigorous filtering process to purge our training data of inappropriate content, such as explicit imagery and offensive language, to minimize the likelihood of generating inappropriate content.

References

- [1] Jie An, Songyang Zhang, Harry Yang, Sonal Gupta, Jia-Bin Huang, Jiebo Luo, and Xi Yin. Latent-shift: Latent diffusion with temporal shift for efficient text-to-video generation. *arXiv preprint arXiv:2304.08477*, 2023. 2
- [2] Omer Bar-Tal, Hila Chefer, Omer Tov, Charles Herrmann, Roni Paiss, Shiran Zada, Ariel Ephrat, Junhua Hur, Guanghui Liu, Amit Raj, et al. Lumiere: A space-time diffusion model for video generation. *arXiv preprint arXiv:2401.12945*, 2024. 6
- [3] Andreas Blattmann, Tim Dockhorn, Sumith Kulal, Daniel Mendelevitch, Maciej Kilian, Dominik Lorenz, Yam Levi, Zion English, Vikram Voleti, Adam Letts, et al. Stable video diffusion: Scaling latent video diffusion models to large datasets. *arXiv preprint arXiv:2311.15127*, 2023. 2, 6
- [4] Andreas Blattmann, Robin Rombach, Huan Ling, Tim Dockhorn, Seung Wook Kim, Sanja Fidler, and Karsten Kreis. Align your latents: High-resolution video synthesis with latent diffusion models. In *CVPR*, 2023. 2
- [5] Haoxin Chen, Menghan Xia, Yingqing He, Yong Zhang, Xiaodong Cun, Shaoshu Yang, Jinbo Xing, Yaofang Liu, Qifeng Chen, Xintao Wang, et al. Videocrafter1: Open diffusion models for high-quality video generation. *arXiv preprint arXiv:2310.19512*, 2023. 2, 11, 12
- [6] Junsong Chen, Jincheng Yu, Chongjian Ge, Lewei Yao, Enze Xie, Yue Wu, Zhongdao Wang, James Kwok, Ping Luo, Huchuan Lu, et al. Pixart- α : Fast training of diffusion transformer for photorealistic text-to-image synthesis. In *ICLR*, 2024. 2, 4, 5
- [7] Mehdi Cherti, Romain Beaumont, Ross Wightman, Mitchell Wortsman, Gabriel Ilharco, Cade Gordon, Christoph Schuhmann, Ludwig Schmidt, and Jenia Jitsev. Reproducible scaling laws for contrastive language-image learning. In *CVPR*, 2023. 4
- [8] Patrick Esser, Sumith Kulal, Andreas Blattmann, Rahim Entezari, Jonas Müller, Harry Saini, Yam Levi, Dominik Lorenz, Axel Sauer, Frederic Boesel, et al. Scaling rectified flow transformers for high-resolution image synthesis. In *ICML*, 2024. 2, 3
- [9] Zhengcong Fei, Mingyuan Fan, Changqian Yu, Debang Li, Youqiang Zhang, and Junshi Huang. Dimba: Transformer-mamba diffusion models. *arXiv preprint arXiv:2406.01159*, 2024. 3
- [10] Rohit Girdhar, Mannat Singh, Andrew Brown, Quentin Duval, Samaneh Azadi, Sai Saketh Rambhatla, Akbar Shah, Xi Yin, Devi Parikh, and Ishan Misra. Emu video: Factorizing text-to-video generation by explicit image conditioning. *arXiv preprint arXiv:2311.10709*, 2023. 2
- [11] Tiankai Hang, Shuyang Gu, Chen Li, Jianmin Bao, Dong Chen, Han Hu, Xin Geng, and Baining Guo. Efficient diffusion training via min-snr weighting strategy. In *ICCV*, 2023. 2, 3
- [12] Jingwen He, Tianfan Xue, Dongyang Liu, Xinqi Lin, Peng Gao, Dahua Lin, Yu Qiao, Wanli Ouyang, and Ziwei Liu. Venhancer: Generative space-time enhancement for video generation. *arXiv preprint arXiv:2407.07667*, 2024. 11, 12
- [13] Jonathan Ho and Tim Salimans. Classifier-free diffusion guidance. *arXiv preprint arXiv:2207.12598*, 2022. 11
- [14] Jonathan Ho, Ajay Jain, and Pieter Abbeel. Denoising diffusion probabilistic models. In *NeurIPS*, 2020. 2, 4
- [15] Wenyi Hong, Ming Ding, Wendi Zheng, Xinghan Liu, and Jie Tang. Cogvideo: Large-scale pretraining for text-to-video generation via transformers. *ICLR*, 2023. 6
- [16] Yaosi Hu, Zhenzhong Chen, and Chong Luo. Lamd: Latent motion diffusion for video generation. *arXiv preprint arXiv:2304.11603*, 2023. 3, 11
- [17] Ziqi Huang, Yanan He, Jiashuo Yu, Fan Zhang, Chenyang Si, Yuming Jiang, Yuanhan Zhang, Tianxing Wu, Qingyang Jin, Nattapol Chanpaisit, et al. Vbench: Comprehensive benchmark suite for video generative models. In *CVPR*, 2024. 6, 12
- [18] Phillip Isola, Jun-Yan Zhu, Tinghui Zhou, and Alexei A Efros. Image-to-image translation with conditional adversarial networks. In *CVPR*, 2017. 11
- [19] Yang Jin, Zhicheng Sun, Ningyuan Li, Kun Xu, Hao Jiang, Nan Zhuang, Quzhe Huang, Yang Song, Yadong Mu, and Zhouchen Lin. Pyramidal flow matching for efficient video generative modeling. *arXiv preprint arXiv:2410.05954*, 2024. 11, 12
- [20] Diederik P Kingma and Max Welling. Auto-encoding variational bayes. In *ICLR*, 2014. 2, 3
- [21] Kuaishou. Kling. <https://kling.kuaishou.com/en>, 2024. 2
- [22] Black Forest Labs. Flux.1. <https://github.com/black-forest-labs/flux>, 2014. 2, 3
- [23] Xingchao Liu, Xiwen Zhang, Jianzhu Ma, Jian Peng, et al. InstafLOW: One step is enough for high-quality diffusion-based text-to-image generation. In *ICLR*, 2023. 3
- [24] Cheng Lu, Yuhao Zhou, Fan Bao, Jianfei Chen, Chongxuan Li, and Jun Zhu. Dpm-solver++: Fast solver for guided sampling of diffusion probabilistic models. *arXiv preprint arXiv:2211.01095*, 2022. 5
- [25] Eric Luhman and Troy Luhman. Knowledge distillation in iterative generative models for improved sampling speed. *arXiv preprint arXiv:2101.02388*, 2021. 3
- [26] Lingchen Meng, Jianwei Yang, Rui Tian, Xiyang Dai, Zuxuan Wu, Jianfeng Gao, and Yu-Gang Jiang. Deepstack: Deeply stacking visual tokens is surprisingly simple and effective for lmms. *arXiv preprint arXiv:2406.04334*, 2024. 5
- [27] Alex Nichol, Prafulla Dhariwal, Aditya Ramesh, Pranav Shyam, Pamela Mishkin, Bob McGrew, Ilya Sutskever, and

- Mark Chen. Glide: Towards photorealistic image generation and editing with text-guided diffusion models. In *ICML*, 2022. 2
- [28] Alexander Quinn Nichol and Prafulla Dhariwal. Improved denoising diffusion probabilistic models. In *ICML*, 2021. 2
- [29] Nvidia. Cosmos tokenizer: A suite of image and video neural tokenizers. <https://github.com/NVIDIA/Cosmos-Tokenizer>, 2024. 5
- [30] Open-Sora. Open-sora. <https://github.com/hpcaitech/Open-Sora>, 2024. 5, 11, 12
- [31] OpenAI. Sora. <https://openai.com/index/sora/>, 2024. 2
- [32] William Peebles and Saining Xie. Scalable diffusion models with transformers. In *ICCV*, 2023. 2, 4
- [33] Pablo Pernias, Dominic Rampas, Mats Leon Richter, Christopher Pal, and Marc Aubreville. Würstchen: An efficient architecture for large-scale text-to-image diffusion models. In *ICLR*, 2024. 3
- [34] Dustin Podell, Zion English, Kyle Lacey, Andreas Blattmann, Tim Dockhorn, Jonas Müller, Joe Penna, and Robin Rombach. Sdxl: Improving latent diffusion models for high-resolution image synthesis. In *ICLR*, 2024. 4, 5, 6
- [35] Adam Polyak, Amit Zohar, Andrew Brown, Andros Tjandra, Animesh Sinha, Ann Lee, Apoorv Vyas, Bowen Shi, Chih-Yao Ma, Ching-Yao Chuang, et al. Movie gen: A cast of media foundation models. *arXiv preprint arXiv:2410.13720*, 2024. 2, 11
- [36] Zhiwu Qing, Shiwei Zhang, Jiayu Wang, Xiang Wang, Yujie Wei, Yingya Zhang, Changxin Gao, and Nong Sang. Hierarchical spatio-temporal decoupling for text-to-video generation. In *CVPR*, 2024. 2
- [37] Colin Raffel, Noam Shazeer, Adam Roberts, Katherine Lee, Sharan Narang, Michael Matena, Yanqi Zhou, Wei Li, and Peter J Liu. Exploring the limits of transfer learning with a unified text-to-text transformer. *JMLR*, 2020. 2, 4
- [38] Danilo Jimenez Rezende, Shakir Mohamed, and Daan Wierstra. Stochastic backpropagation and approximate inference in deep generative models. In *ICML*, 2014. 2
- [39] Iain E Richardson. *The H. 264 advanced video compression standard*. John Wiley & Sons, 2011. 3
- [40] Robin Rombach, Andreas Blattmann, Dominik Lorenz, Patrick Esser, and Björn Ommer. High-resolution image synthesis with latent diffusion models. In *CVPR*, 2022. 2, 3, 4, 5, 11
- [41] Joanne K Rowling. *Harry Potter and the goblet of fire*. Bloomsbury publishing, 2019. 2
- [42] Runway. Gen-3. <https://runwayml.com/research/introducing-gen-3-alpha>, 2024. 2
- [43] Uriel Singer, Adam Polyak, Thomas Hayes, Xi Yin, Jie An, Songyang Zhang, Qiuyuan Hu, Harry Yang, Oron Ashual, Oran Gafni, et al. Make-a-video: Text-to-video generation without text-video data. *ICLR*, 2023. 6
- [44] Yang Song, Jascha Sohl-Dickstein, Diederik P Kingma, Abhishek Kumar, Stefano Ermon, and Ben Poole. Score-based generative modeling through stochastic differential equations. In *ICLR*, 2021. 2
- [45] Yang Song, Prafulla Dhariwal, Mark Chen, and Ilya Sutskever. Consistency models. In *ICML*, 2023. 2, 3
- [46] Khurram Soomro, Amir Roshan Zamir, and Mubarak Shah. Ucf101: A dataset of 101 human actions classes from videos in the wild. *arXiv preprint arXiv:1212.0402*, 2012. 6
- [47] Haotian Tang, Yecheng Wu, Shang Yang, Enze Xie, Junsong Chen, Junyu Chen, Zhuoyang Zhang, Han Cai, Yao Lu, and Song Han. Hart: Efficient visual generation with hybrid autoregressive transformer. *arXiv preprint arXiv:2410.10812*, 2024. 3
- [48] Yao Teng, Yue Wu, Han Shi, Xuefei Ning, Guohao Dai, Yu Wang, Zhenguo Li, and Xihui Liu. Dim: Diffusion mamba for efficient high-resolution image synthesis. *arXiv preprint arXiv:2405.14224*, 2024. 2, 3
- [49] Thomas Unterthiner, Sjoerd Van Steenkiste, Karol Kurach, Raphael Marinier, Marcin Michalski, and Sylvain Gelly. Towards accurate generative models of video: A new metric & challenges. *arXiv preprint arXiv:1812.01717*, 2018. 5
- [50] Junke Wang, Yi Jiang, Zehuan Yuan, Binyue Peng, Zuxuan Wu, and Yu-Gang Jiang. Omnitokenizer: A joint image-video tokenizer for visual generation. *arXiv preprint arXiv:2406.09399*, 2024. 5
- [51] Wenjing Wang, Huan Yang, Zixi Tuo, Huiguo He, Junchen Zhu, Jianlong Fu, and Jiaying Liu. Videofactory: Swap attention in spatiotemporal diffusions for text-to-video generation. *arXiv preprint arXiv:2305.10874*, 2023. 2
- [52] Yanhui Wang, Jianmin Bao, Wenming Weng, Ruoyu Feng, Dacheng Yin, Tao Yang, Jingxu Zhang, Qi Dai, Zhiyuan Zhao, Chunyu Wang, et al. Microcinema: A divide-and-conquer approach for text-to-video generation. In *CVPR*, 2024. 2, 6
- [53] Yaohui Wang, Xinyuan Chen, Xin Ma, Shangchen Zhou, Ziqi Huang, Yi Wang, Ceyuan Yang, Yanan He, Jiashuo Yu, Peiqing Yang, et al. Lavie: High-quality video generation with cascaded latent diffusion models. *IJCV*, 2024. 2, 6, 11, 12
- [54] Zhou Wang, Alan C Bovik, Hamid R Sheikh, and Eero P Simoncelli. Image quality assessment: from error visibility to structural similarity. *IEEE TIP*, 2004. 5
- [55] Zhendong Wang, Yifan Jiang, Huangjie Zheng, Peihao Wang, Pengcheng He, Zhangyang Wang, Weizhu Chen, Mingyuan Zhou, et al. Patch diffusion: Faster and more data-efficient training of diffusion models. *NeurIPS*, 2024. 2, 3
- [56] Enze Xie, Junsong Chen, Junyu Chen, Han Cai, Yujun Lin, Zhekai Zhang, Muyang Li, Yao Lu, and Song Han. Sana: Efficient high-resolution image synthesis with linear diffusion transformers. *arXiv preprint arXiv:2410.10629*, 2024. 3
- [57] Jinbo Xing, Menghan Xia, Yong Zhang, Haoxin Chen, Wangbo Yu, Hanyuan Liu, Gongye Liu, Xintao Wang, Ying Shan, and Tien-Tsin Wong. Dynamicrafter: Animating open-domain images with video diffusion priors. In *ECCV*, 2024. 2, 6
- [58] Zhen Xing, Qi Dai, Han Hu, Zuxuan Wu, and Yu-Gang Jiang. Simda: Simple diffusion adapter for efficient video generation. In *CVPR*, 2024. 2

- [59] Zhen Xing, Qijun Feng, Haoran Chen, Qi Dai, Han Hu, Hang Xu, Zuxuan Wu, and Yu-Gang Jiang. A survey on video diffusion models. *ACM Computing Surveys*, 2024. 2
- [60] Jun Xu, Tao Mei, Ting Yao, and Yong Rui. Msr-vtt: A large video description dataset for bridging video and language. In *CVPR*, 2016. 6
- [61] Yanwu Xu, Yang Zhao, Zhisheng Xiao, and Tingbo Hou. Ufogen: You forward once large scale text-to-image generation via diffusion gans. In *CVPR*, 2024. 2, 3
- [62] Zhuoyi Yang, Jiayan Teng, Wendi Zheng, Ming Ding, Shiyu Huang, Jiazheng Xu, Yuanming Yang, Wenyi Hong, Xiaohan Zhang, Guanyu Feng, et al. Cogvideox: Text-to-video diffusion models with an expert transformer. *arXiv preprint arXiv:2408.06072*, 2024. 2
- [63] Sihyun Yu, Kihyuk Sohn, Subin Kim, and Jinwoo Shin. Video probabilistic diffusion models in projected latent space. In *CVPR*, 2023. 3
- [64] Sihyun Yu, Weili Nie, De-An Huang, Boyi Li, Jinwoo Shin, and Anima Anandkumar. Efficient video diffusion models via content-frame motion-latent decomposition. In *ICLR*, 2024. 3
- [65] Yan Zeng, Guoqiang Wei, Jiani Zheng, Jiaxin Zou, Yang Wei, Yuchen Zhang, and Hang Li. Make pixels dance: High-dynamic video generation. In *CVPR*, 2024. 2
- [66] David Junhao Zhang, Jay Zhangjie Wu, Jia-Wei Liu, Rui Zhao, Lingmin Ran, Yuchao Gu, Difei Gao, and Mike Zheng Shou. Show-1: Marrying pixel and latent diffusion models for text-to-video generation. *IJCV*, 2024. 2, 6, 11, 12
- [67] Richard Zhang, Phillip Isola, Alexei A Efros, Eli Shechtman, and Oliver Wang. The unreasonable effectiveness of deep features as a perceptual metric. In *CVPR*, 2018. 5
- [68] Richard Zhang, Phillip Isola, Alexei A Efros, Eli Shechtman, and Oliver Wang. The unreasonable effectiveness of deep features as a perceptual metric. In *CVPR*, 2018. 11
- [69] Xuanlei Zhao, Xiaolong Jin, Kai Wang, and Yang You. Real-time video generation with pyramid attention broadcast. *arXiv preprint arXiv:2408.12588*, 2024. 3

A. Implementation details

Reducio-VAE. We demonstrate the detailed architecture of *Reducio* in Fig. 8. Generally, we follow the training strategies of SD-VAE [40]. We employ a tailored version of PatchGAN [18] based on 3D convolutions and optimize the model with L_1 loss, KL loss, perceptual loss [68], and GAN loss. While initializing the 2D encoder and the 3D VAE with SD-VAE pre-trained weights accelerates convergence, we find that freezing the 2D encoder leads to worse performance than training the full parameters. We follow LaMD [16] to feed the motion latent into a normalization layer to obtain the output of the VAE encoder. Therefore, in the stage of diffusion training, we use a scale factor of 1.0, which is multiplied by the input latent as inputs into DiT.

During inference, We split videos with a resolution over 256×256 into overlapping spatial tiles, we fuse the encoded latent as well as the video output, in a similar manner with

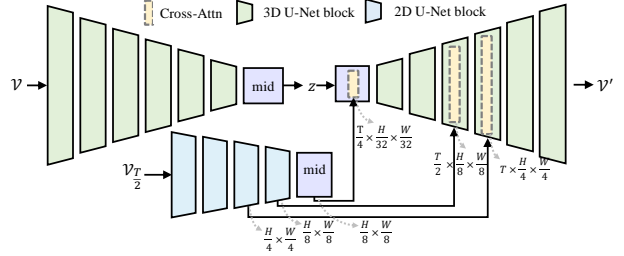


Figure 8. The detailed architecture of *Reducio*-VAE with $f_t = 4$, $f_s = 32$.

Table 9. Hyperparameters for *Reducio*-VAE

<i>Reducio</i> -VAE		
z -shape [†]	$4 \times 8 \times 8 \times 16$	$8 \times 8 \times 8 \times 16$
Channels (3d)	128	
Channels (2d)	128	
Ch Multiplier (3d)	1,2,2,4,4,4	
Ch Multiplier (2d)	1,2,2,4,4	
Depth	2	
Batch size	32	24
Learning rate	4e-5	
Iterations	1,000,000	

Table 10. Comparison with more SOTA models on Vbench.

Model	Quality Score	Semantic Score	Total Score
Show-1 [66]	80.42	72.98	78.93
Lavie [53]	78.78	70.31	77.08
VideoCrafter [5]	81.59	72.22	79.72
OpenSora v1.2 [30]	81.35	73.39	79.76
Lavie-2 [53]	83.24	75.76	81.75
Pyramid Flow [19]	84.74	69.62	81.72
VideoCrafter-2 [12]	83.27	76.73	81.97
Reducio-DiT	82.24	78.00	81.39

Movie Gen [35]. Note that since *Reducio*-VAE employs a spatial down-sampling factor of 32, *Reducio*-VAE can only process video inputs whose width and height are divisible by 32. Otherwise, videos should be padded to meet this requirement before being fed into the VAE.

Reducio-DiT. We elaborate on the details of content image conditions in Fig. 9. During inference, we use classifier-free guidance [13] for better generation quality and set the default scale to 2.5. During training, we randomly drop image conditions at a probability of 0.1, as well as drop 10% text conditions.

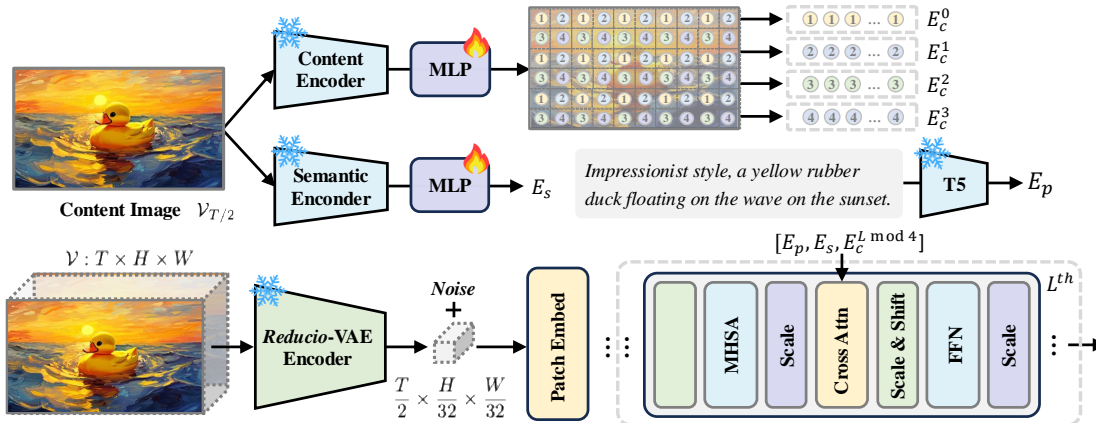


Figure 9. The overview of the efficient content condition solution for *Reducio*-DiT on high-resolution videos.

Table 11. Detailed quantitative comparison with SOTA for text-to-video generation models on VBench.

Model	subject consistency	background consistency	temporal flickering	motion smoothness	dynamic degree	aesthetic quality	imaging quality	object class	multiple objects	human action	color	spatial relationship	scene	appearance style	temporal style	overall consistency
Lavie [53]	91.41	97.47	98.30	96.38	49.72	54.94	61.90	91.82	33.32	96.80	86.39	34.09	52.69	23.56	25.93	26.41
Show-1 [66]	95.53	98.02	99.12	98.24	44.44	57.35	58.66	93.07	45.47	95.60	86.35	53.50	47.03	23.06	25.28	27.46
VideoCrafter [5]	95.10	98.04	98.93	95.67	55.00	62.67	65.46	78.18	45.66	91.60	93.32	58.86	43.75	24.41	25.54	26.76
OpenSora v1.2 [30]	96.75	97.61	99.53	98.50	42.39	56.85	63.34	82.22	51.83	91.20	90.08	68.56	42.44	23.95	24.54	26.85
Lavie-2 [53]	97.90	98.45	98.76	98.42	31.11	67.62	70.39	97.52	64.88	96.40	91.65	38.68	49.59	25.09	25.24	27.39
Pyramid Flow [19]	96.95	98.06	99.49	99.12	64.63	63.26	65.01	86.67	50.71	85.60	82.87	59.53	43.20	20.91	23.09	26.23
VideoCrafter-2 [12]	97.17	98.54	98.46	97.75	42.50	65.89	70.45	93.39	49.83	95.00	94.41	64.88	51.82	24.32	25.17	27.57
Reducio-DiT	98.05	99.13	98.45	98.77	27.78	64.02	67.67	91.49	69.91	92.60	89.06	52.85	54.90	25.16	26.40	28.87

B. Additional results

We display the detailed performance comparison on VBench [17] in Tab. 11 and Tab. 10. As the results show, *Reducio*-DiT achieves a promising semantic score of 78.00, beating a range of state-of-the-art LDMs.